North Atlantic ventilation of "southern-sourced" deep water in the glacial ocean

Eun Young Kwon,[1] Mathis P. Hain,[2] Daniel M. Sigman,[2] Eric D. Galbraith,[3] Jorge L. Sarmiento,[4] and J. R. Toggweiler[5]

Received 9 August 2011; revised 2 April 2012; accepted 13 April 2012; published 23 May 2012.

[1] One potential mechanism for lowering atmospheric CO_2 during glacial times is an increase in the fraction of the global ocean ventilated by the North Atlantic, which produces deep water with a low concentration of unused nutrients and thus drives the ocean's biological pump to a high efficiency. However, the data indicate that during glacial times, a water mass low in $^{13}C/^{12}C$ and $^{14}C/C$ occupied the deep Atlantic, apparently at the expense of North Atlantic Deep Water (NADW). This water is commonly referred to as "southern-sourced" because of its apparent entry into the Atlantic basin from the South, prompting the inference that it was ventilated at the Southern Ocean surface. Here, we propose that this deep Atlantic water mass actually included a large fraction of North Atlantic-ventilated water, the chemical characteristics of which were altered by recirculation in the deep Southern and Indo-Pacific oceans. In an ocean model sensitivity experiment that reduces Antarctic Bottom Water formation and weakens its overturning circulation, we find that a much greater fraction of NADW is transported into the Southern Ocean without contacting the surface and is entrained and mixed into the southern-sourced deep water that spreads into the global abyssal ocean. Thus, North Atlantic ventilation takes over more of the ocean interior, lowering atmospheric CO_2, and yet the abyssal Atlantic is filled from the South with old water low in $^{13}C/^{12}C$ and $^{14}C/C$, consistent with glacial data.

Citation: Kwon, E. Y., M. P. Hain, D. M. Sigman, E. D. Galbraith, J. L. Sarmiento, and J. R. Toggweiler (2012), North Atlantic ventilation of "southern-sourced" deep water in the glacial ocean, *Paleoceanography*, *27*, PA2208, doi:10.1029/2011PA002211.

1. Introduction

[2] The changes in atmospheric CO_2 over glacial/interglacial cycles of the late Pleistocene are at least partly due to coupled changes in the biogeochemistry and circulation of the ocean [*Sarmiento and Toggweiler*, 1984; *Knox and McElroy*, 1984; *Siegenthaler and Wenk*, 1984; *Broecker and Peng*, 1987; *Toggweiler*, 1999; *Sigman and Boyle*, 2000; *Archer et al.*, 2003; *Toggweiler et al., 2003*; *Sigman and Haug*, 2003; *Köhler and Fischer*, 2006; *Marinov et al.*, 2008a, 2008b; *Sigman et al.*, 2010; *Hain et al.*, 2010; *Kwon et al.*, 2011], and the interactions of the Southern Ocean and North Atlantic are likely central to these changes [*Archer et al.*, 2003; *Sigman et al.*, 2010]. The role of these two regions of deep water formation in the ocean storage of CO_2 can be understood in terms of "preformed" versus "regenerated" nutrients, where "regenerated" nutrients are those used by organisms in the surface ocean to build soft-tissue organic matter that rains into the ocean interior before being respired, thereby sequestering carbon away from the atmosphere, whereas "preformed" nutrients enter the ocean interior dissolved in the descending water, without being used in the production of organic matter, and thus track the inefficiency of the soft-tissue pump [*Broecker et al.*, 1985; *Takahashi et al.*, 1985; *Redfield*, 1942; *Anderson and Sarmiento*, 1994]. The modern Antarctic Zone of the Southern Ocean has the highest concentration of surface nutrients, forms deep water that is rich in preformed nutrients, and therefore constitutes the principle leak in the global soft-tissue pump [*Toggweiler et al.*, 2003; *Sarmiento and Toggweiler*, 1984; *Knox and McElroy*, 1984; *Siegenthaler and Wenk*, 1984]. Thus, the global efficiency of the soft-tissue pump and the level of atmospheric CO_2 are extremely sensitive to the relative volumes of the deep ocean last ventilated in the North Atlantic versus the Southern Ocean [*Sigman and Haug*, 2003; *Toggweiler et al.*, 2003; *Ito and Follows*, 2005; *Marinov et al.*, 2008b; *Schmittner and*

[1]Department of Atmospheric and Oceanic Sciences, University of California, Los Angeles, California, USA.
[2]Department of Geosciences, Princeton University, Princeton, New Jersey, USA.
[3]Earth and Planetary Sciences, McGill University, Montreal, Quebec, Canada.
[4]Atmospheric and Oceanic Sciences Program, Princeton University, Princeton, New Jersey, USA.
[5]Geophysical Fluid Dynamics Laboratory, National Oceanic and Atmospheric Administration, Princeton, New Jersey, USA.

Corresponding author: E. Y. Kwon, Department of Atmospheric and Oceanic Sciences, University of California, 405 Hilgard Ave., 7127 Math Sciences Bldg., Los Angeles, CA 90095, USA. (ekwon@atmos.ucla.edu)

Copyright 2012 by the American Geophysical Union.
0883-8305/12/2011PA002211

Galbraith, 2008; *Hain et al.*, 2010; *Kwon et al.*, 2011]. Ocean circulation/mixing determines the relative volumetric importance of these different regions of deep water formation.

[3] The "stratification" hypothesis for lower glacial atmospheric CO_2 levels, as framed by *François et al.* [1997], posits that upper ocean stratification around Antarctica slowed the rate at which nutrient-rich and carbon-rich deep water was brought to the surface, reducing the evasion of CO_2 to the atmosphere. Model studies simulating Antarctic stratification uniformly project a decline in atmospheric CO_2, for which there are two separable causes. First, Antarctic stratification reduces the volume of water in the ocean interior that originated from ventilation in the Southern Ocean surface, thereby replacing southern-ventilated water that is rich in preformed nutrients with North Atlantic-ventilated water characterized by low preformed nutrient concentrations [*Toggweiler et al.*, 2003; *Marinov et al.*, 2008b]. Second, depending on the parameterization of export production used in a given model, Antarctic export production may not decline as much as the gross nutrient supply from below [*François et al.*, 1997]. In this case, Antarctic surface nutrient concentration decreases, lowering the preformed nutrient content of Southern Ocean-ventilated deep water [*Sarmiento and Toggweiler*, 1984]. Given ongoing uncertainty in how Antarctic surface nutrients changed during glacial times (compare *Robinson and Sigman* [2008] with *Elderfield and Rickaby* [2000]), it is of particular importance to assess how much of the glacial-interglacial CO_2 change may have been caused by the "ventilation volume" mechanism alone, that is, the glacial expansion of ocean volume last ventilated from the North Atlantic.

[4] However, reconstructions of water mass geometry in the Atlantic Ocean during the last glacial maximum (LGM) appear to argue against the "ventilation volume" aspect of the stratification hypothesis. According to chemical proxy evidence, southern-sourced bottom water expanded and North Atlantic Deep Water (NADW) penetrated only to mid-depths of the Atlantic Ocean [*Boyle and Keigwin*, 1987; *Duplessy et al.*, 1988; *Curry and Oppo*, 2005; *Lynch-Stieglitz et al.*, 2007; *Skinner*, 2009]. If the southern-sourced bottom water occupying both the deep Atlantic and the deep Indo-Pacific was almost entirely ventilated by the Southern Ocean, with close to its modern burden of preformed nutrients, then atmospheric CO_2 should have increased [*Toggweiler et al.*, 2003; *Marinov et al.*, 2008b, *Hain et al.*, 2010; *Kwon et al.*, 2011], counter to observations [*Petit et al.*, 1999]. Two ways out of this paradox of observed expansion of the southern-sourced bottom water and concurrent atmospheric CO_2 decline have already been identified: (1) increased nutrient consumption in Antarctic surface waters, as described above [e.g., *Robinson and Sigman*, 2008; *Sarmiento and Toggweiler*, 1984; *Knox and McElroy*, 1984; *Siegenthaler and Wenk*, 1984], or (2) the prevention of CO_2 escape out of Antarctic surface waters due to extensive sea ice cover [e.g., *Stephens and Keeling*, 2000].

[5] In this study, we revisit the plausibility that a ventilation volume change played a role in lowering atmospheric CO_2 during glacial times. We show that glacial southern-sourced deep water may have included a large fraction of entrained NADW, lowering the preformed nutrient content of the global ocean and thus increasing the ocean sequestration of respired carbon. This entrainment does not contradict the evidence that abyssal Atlantic water was dominated by an expanded "southern-sourced" water mass [e.g., *Curry and Oppo*, 2005; *Marchitto and Broecker*, 2006; *Robinson et al.*, 2005; *Rutberg et al.*, 2000; *Piotrowski et al.*, 2005], flowing into the Atlantic basin from the high latitude Southern Hemisphere [*Hain et al.*, 2010]. Based on box model results, *Hain et al.* [2010] proposed that greater North Atlantic ventilation of the glacial ocean is required to explain the low glacial CO_2 levels, and that such a scenario would be consistent with the observed glacial distribution of carbon isotopes in the ocean.

[6] In the present-day ocean, the "southern-sourced" deep water has two ventilation regions, with one dominating: it is comprised primarily of water last exposed to the Southern Ocean mixed layer ("Southern Ocean-ventilated" water), with a much smaller contribution from water last exposed to the North Atlantic mixed layer ("North Atlantic-ventilated" water) [*Broecker et al.*, 1998; *Johnson*, 2008; *Gebbie and Huybers*, 2010; *Gebbie and Huybers*, 2011; *DeVries and Primeau*, 2011]. The Southern Ocean-ventilated fraction includes very dense bottom water formed on the continental shelf of Antarctica [*Price and Baringer*, 1994] and water transformed into a dense class of Antarctic Bottom Water in the Southern Ocean mixed layer [*Orsi et al.*, 1999; *Iudicone et al.*, 2008]. Part of this Southern Ocean-ventilated water derives from NADW that enters the Southern Ocean and is re-ventilated under Southern Ocean conditions, thereby becoming "Southern Ocean-ventilated" water. There is a small remnant "North Atlantic-ventilated" fraction comprised of NADW that is internally entrained and mixed into the southern-sourced water, without being exposed to the atmosphere in the Southern Ocean [e.g., *Speer et al.*, 2000; *Iudicone et al.*, 2008; *Broecker et al.*, 1985]. This internal water mass transformation, caused by cross-isopycnal diffusive fluxes below the mixed layer [*Walin*, 1982; *Tziperman*, 1986], cabbeling and thermobaricity [*Downes et al.*, 2011], allows the "North Atlantic-ventilated, southern-sourced" deep water to retain the preformed chemical signature acquired from the North Atlantic mixed layer, although its physical and biogeochemical properties have been altered by diffusion and recirculation within the ocean's interior. With reduced upwelling and convection in the glacial Southern Ocean, the re-ventilation of northern-sourced deep waters within the Southern Ocean may have been minimized. Under this condition, we propose that the subsurface entrainment of "North Atlantic-ventilated" water into "southern-sourced" deep water became proportionally more important, causing "southern-sourced" deep water to transition away from being predominantly "Southern Ocean-ventilated" toward being more "North Atlantic-ventilated."

[7] Below, we explore whether our hypothesized glacial ocean—the stratified deep ocean filled with the southern-sourced deep water dominantly ventilated from the North Atlantic—is consistent with data on the carbon chemistry of the deep ocean. To this end, we use two idealized circulation models: simulation 1 where the southern-sourced deep water is mostly ventilated from the Southern Ocean (Southern Ocean ventilation scenario) and simulation 2 where the Southern Ocean overturning circulation slows down relative to simulation 1 and, largely as a consequence of this change,

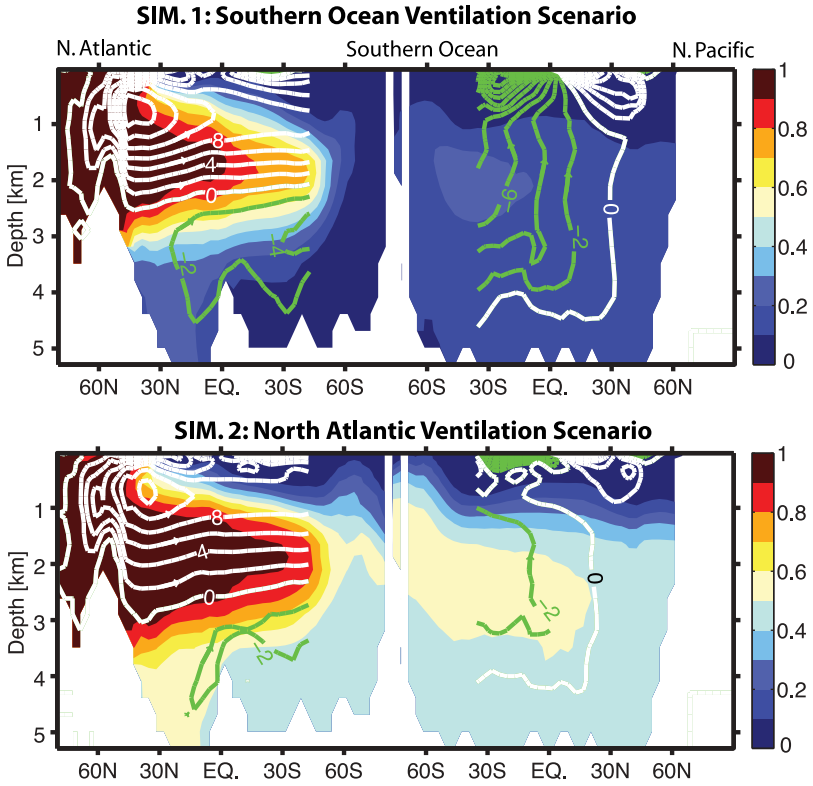

Figure 1. Ocean circulation patterns. Color shade represents the fraction of the ocean ventilated from the northern North Atlantic (north of 40°N). Zonally averaged fields for the Atlantic and Indo-Pacific are shown. The transect runs from the North Atlantic on the left through the Southern Ocean in the middle and to the North Pacific on the right. Contour interval is 0.1. Solid line represents the stream function of the meridional overturning circulation for the Atlantic Ocean and the Indo-Pacific Oceans. The arrow heads indicate the sense of circulation. Contour interval is 2 Sv (1 Sv = 10^6 m^3 s^{-1}).

the southern-sourced water becomes dominantly ventilated from the North Atlantic (North Atlantic ventilation scenario). As will be shown below, this sensitivity experiment of the two idealized simulations reveals that the differences in the air-sea distributions of carbon and its isotopes ($^{13}C/^{12}C$ and $^{14}C/C$) are consistent with some of the key aspects of the observed glacial/interglacial changes, supporting our hypothesis.

2. Simulations of Ocean Circulation and Atmospheric CO_2

[8] We adopt two circulation models from *DeVries and Primeau* [2009] and *Kwon et al.* [2011] to represent the Southern Ocean ventilation scenario (simulation 1 hereafter) and the North Atlantic ventilation scenario (simulation 2 hereafter). The choice of these two simulations is motivated by the substantial CO_2 drawdown in simulation 2 relative to simulation 1 [*Kwon et al.*, 2011], which results from the change in the global ocean ventilation pattern close to our hypothesized glacial change. Simulation 1 was regarded as the control model in the two previous studies and has the southern-sourced deep water dominantly ventilated from the Southern Ocean like the present-day ocean [*Primeau*, 2005; *Broecker et al.*, 1998; *Johnson*, 2008; *Gebbie and Huybers*, 2010, 2011; *DeVries and Primeau*, 2011]. Despite a rather shallow depth of NADW in the Atlantic basin, the good agreement in the ventilation pattern of the global ocean between simulation 1 and observation-based estimates of the modern ocean underscores that simulation 1 is an appropriate interglacial representation (compare Figure 1 with Figures 8–10 in *Gebbie and Huybers* [2010], or alternatively compare Figures 4–6 in *Primeau* [2005] with Figures 8–10 in *Gebbie and Huybers* [2010]). Simulation 2, which is obtained by reducing the vertical diffusivity coefficient from 0.5 cm^2 s^{-1} to 0.15 cm^2 s^{-1} globally, has a reduced Southern Ocean overturning circulation, with its southern-sourced deep water containing a greater volume fraction of North Atlantic ventilated water compared to simulation 1 (Figure 1). We note that the two simulations in themselves are better representatives of the two end-members of deep ocean ventilation (Southern Ocean- versus North Atlantic-ventilated) than of the interglacial and glacial oceans. Nevertheless, as will be described below, simulated atmospheric CO_2, oceanic $^{13}C/^{12}C$, $^{14}C/C$ and oxygen distributions of simulations 1 and 2 fit with observations of the Holocene and the LGM ocean, respectively, and therefore we compare our simulations in that context. While both simulations undoubtedly miss many features of both climate states, including realistic glacial boundary forcing (see section 4), our core hypothesis is that the contrasts between the two scenarios encapsulate a fundamental difference in deep ocean ventilation between interglacial and glacial times.

[9] Both simulations are generated from a coarse resolution ocean general circulation model where subgrid scale

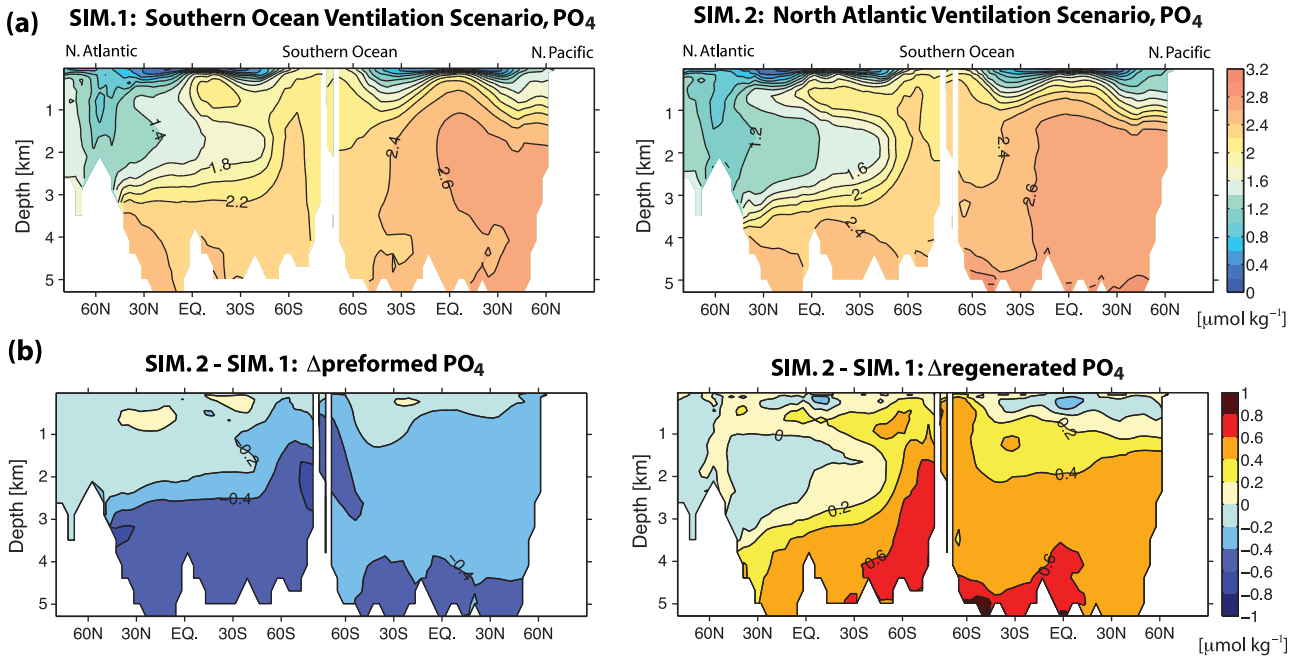

Figure 2. Phosphate distributions. (a) Zonally averaged concentrations of PO_4 along the Atlantic and Pacific oceans (μmol kg^{-1}). (b) Differences in preformed PO_4 (left panel) and regenerated PO_4 (right panel) between simulation 2 and simulation 1. The zonally averaged fields run from the North Atlantic on the left through the Southern Ocean in the middle to the North Pacific on the right.

mixing is parameterized using the KPP vertical mixing scheme [*Large et al.*, 1994] and the GM isopycnal eddy-mixing scheme [*Gent and McWilliams*, 1990]. The ocean circulation model is fully integrated to equilibrium under the pre-industrial atmospheric forcing, and the annual mean velocity and mixing tensor fields are taken to the off-line ocean biogeochemistry model of *Kwon and Primeau* [2008]. The ocean biogeochemistry model is based on the second phase of the Ocean Carbon Model Intercomparison Project (OCMIP-II) [*Najjar et al.*, 2007] and has phosphate, alkalinity, oxygen, ^{12}C, ^{13}C and ^{14}C as prognostic tracers. We add a one box model of the atmosphere to the 3-D ocean biogeochemistry model in order to examine the air-sea partitioning of carbon and its isotopes. We refer readers to *Primeau* [2005] for details of the ocean transport model and *Kwon and Primeau* [2008] for details of the biogeochemistry model used herein, and its evaluation against the climatology data of ocean biogeochemical tracers.

[10] The dominant driver of differences in the two simulations is the low rate of Southern Ocean overturning in simulation 2: the overturning rate of the southern-sourced bottom water decreases from 11 Sv in simulation 1 to 5 Sv in simulation 2, while the overturning rate of the northern-sourced water decreases only modestly from 15 Sv to 13 Sv [*Kwon et al.*, 2011]. As a result of their difference in Southern Ocean overturning rate, the fractions of the global ocean ventilated from the North Atlantic and Southern Ocean are starkly different in the two simulations (Figure 1). Below, we refer to "North Atlantic-ventilated water" (ocean interior water ventilated north of 40°N in the North Atlantic) as NADW and "Southern Ocean-ventilated water" (ocean interior water ventilated south of 50°S) as AABW. Note that although our definition of AABW is based on the ventilation region of the entire Southern Ocean, most of AABW is formed in the Weddell Sea, the Atlantic sector of the Southern Ocean, as shown in Figure 1 [see also *Primeau*, 2005]. In simulation 1, strong convective mixing brings Circumpolar Deep Water (CDW), which is a mixture of NADW and AABW, to the surface south of the polar front, the surface region from which AABW derives. In contrast, in simulation 2, the enhanced stratification of the Southern Ocean and resulting reduced convective mixing allows NADW to be transported southwards in the Atlantic and around the Southern Ocean with little or no contact with the surface. As a result, a significant fraction of NADW is entrained and mixed into the southern-sourced deep water, and subsequently fills the global deep ocean without being converted into AABW. The net effect is that changing from simulation 1 to simulation 2 increases the fraction of the global ocean last ventilated by the North Atlantic from 21% to 44% at the expense of Southern Ocean ventilation, which decreases from 62% to 39%. Most of the ventilation source change occurs in the vast deep Indo-Pacific, where the contribution of North Atlantic-ventilated water roughly triples (Figure 1).

[11] The two simulations yield nearly identical nutrient distributions (Figure 2a), but this similarity belies substantial differences in biogeochemistry and carbon cycling. Due largely to the increased ocean volume ventilated from the North Atlantic, the preformed nutrient content in the global ocean decreases from 1.50 μmol kg^{-1} in simulation 1 to 1.20 μmol kg^{-1} in simulation 2 (Figure 2b). This reduction in preformed nutrients is necessarily accompanied by an increase in the oceanic storage of respired carbon and a decrease in atmospheric CO_2 [e.g., *Ito and Follows*, 2005]. A similar shift from preformed to remineralized nutrients

during the glacial was inferred from the authigenic uranium content of glacial pelagic sediments [*François et al.*, 1997; *Galbraith et al.*, 2007; *Jaccard et al.*, 2009; *Bradtmiller et al.*, 2010]. While the net CO_2 decline of 32 ppm in these simulations depends on the air-sea gas exchange and the biological/solubility pumps [*Kwon et al.*, 2011], the ventilation volume change causes by itself a 45 ppm reduction (see the Appendix section), representing an increase in the global efficiency of the biological pump.

3. Simulations of Carbon Isotopes

[12] To examine the degree to which our idealized circulation change affects ocean chemical tracers, we implement ^{13}C and a simple ^{14}C-like tracer in the model. The cycling of ^{13}C is simulated in the same way as the cycling of ^{12}C, but taking into account isotope fractionation during air-sea carbon exchange and photosynthesis. We follow *Lynch-Stieglitz et al.* [1995] for the fractionation factors during air-sea ^{13}C exchange, and assume that a fractionation of -20 permil occurs during the production of organic carbon [*Broecker and Maier-Reimer*, 1992]. The $\delta^{13}C$ is obtained based on simulated ^{12}C and ^{13}C as

$$\delta^{13}C = 10^3 \left(\frac{\left(\frac{^{13}C}{^{12}C}\right)_{sample}}{\left(\frac{^{13}C}{^{12}C}\right)_{standard}} - 1 \right), \quad (1)$$

where $(^{13}C/^{12}C)_{standard} = 0.0112$ [*International Union of Pure and Applied Chemistry*, 1999]. The total amount of ^{13}C in the ocean-atmosphere system is determined such that atmospheric $\delta^{13}C$ in simulation 1 is the pre-industrial atmospheric value of -6.48 permil. The resulting total amount of ^{13}C, which makes up 1.11% of total carbon ($^{12}C + {}^{13}C$), is then held fixed throughout the simulations.

[13] We also implement a simple ^{14}C-like tracer, which decays in the ocean's interior with a half-life of 5730 years. The $\Delta^{14}C$ is obtained based on simulated ^{14}C, ^{13}C and ^{12}C as

$$\Delta^{14}C = 10^3 \left(\frac{\left(\frac{^{14}C}{C}\right)_{sample}}{\left(\frac{^{14}C}{C}\right)_{standard}} - 1 \right), \quad (2)$$

where $(^{14}C/C)_{standard} = 1.176 \times 10^{-12}$ is the ratio of ^{14}C to C in the preindustrial atmosphere [*Olsson*, 1970]; $(^{14}C/C)_{sample}$ is the ^{13}C corrected measure of the ^{14}C activity, following *Stuiver and Polach* [1977]:

$$\left(\frac{^{14}C}{C}\right)_{sample} = \left(\frac{^{14}C}{^{12}C}\right)_{sample} \left(1 - \frac{2(25 + \delta^{13}C)}{1000}\right). \quad (3)$$

The atmospheric production rate of ^{14}C is determined such that the atmospheric $\Delta^{14}C$ in simulation 1 is 0 permil. The resulting production rate of 382 moles per year is kept constant between simulations 1 and 2. With the production rate being held constant, atmospheric ^{14}C is determined by the balance between the constant source in the atmosphere and its net flux into the ocean.

[14] From simulation 1 to simulation 2, the $\delta^{13}C$ of dissolved inorganic carbon in deep waters declines due to the accumulation of more respired carbon (Figures 2 and 3). The oceanic storage of respired carbon increases from 91 μmol kg^{-1} in simulation 1 to 134 μmol kg^{-1} in simulation 2 despite a decrease in the globally integrated export production of particulate organic carbon from 15 Pg C yr^{-1} to 9 Pg C yr^{-1}. In the model, ocean productivity varies so as to maintain the same surface nutrient field in simulations 1 and 2, so the increased carbon storage cannot be attributed to an increase in surface nutrient consumption in any one region. Rather, the increased carbon storage is driven by a decrease in the fraction of abyssal water ventilated from the (high preformed nutrient) Antarctic surface and an increase in the fraction ventilated from the (low preformed nutrient) North Atlantic surface. Similar to observations [e.g., *Ninnemann and Charles*, 2002; *Curry and Oppo*, 2005; *Toggweiler et al.*, 2006; *Lisiecki*, 2010], a pronounced reduction in $\delta^{13}C$ occurs in the southern-sourced deep water, especially in the Atlantic sector of the Southern Ocean, where a considerable amount of preformed nutrient is replaced with regenerated nutrient (Figure 2).

[15] We highlight the relatively large change in simulated $\delta^{13}C$, in contrast to the very small change in PO_4; this shows how strongly these two tracers can be decoupled by a change in ocean circulation and warns against interpreting $\delta^{13}C$ as a "nutrient" tracer. For example, the change in deep ocean $\delta^{13}C$ from simulation 1 to simulation 2 is poorly scaled with the change in PO_4 (Figure 4). Instead, the deep ocean $\delta^{13}C$ change is closely related to the biological sequestration of carbon (i.e., the change in regenerated PO_4) such that $\delta^{13}C$ declines largely because preformed PO_4 is converted into regenerated PO_4, without change in the absolute concentration of PO_4.

[16] From simulation 1 to simulation 2, atmospheric $\Delta^{14}C$ rises from 0 to 130 permil without any change in the simulated ^{14}C production rate. At the same time, the global deep and bottom waters become lower in $^{14}C/C$, enhancing the vertical contrast in the radiocarbon content between the ocean and atmosphere, roughly consistent with observations for the glacial Atlantic and Southern Ocean [*Robinson et al.*, 2005; *Skinner et al.*, 2010; *Thornalley et al.*, 2011; *Burke and Robinson*, 2012]. This rearrangement of $\Delta^{14}C$ results from the reductions in the rates at which southern- and northern-ventilated waters enter the deep ocean recharged with ^{14}C. Instead of being recharged with ^{14}C at the Southern Ocean surface, a greater fraction of NADW is internally mixed and entrained into the southern-sourced deep water. This switch from convection to deep entrainment drives a substantial aging of the global abyssal ocean. The average ventilation age of deep water south of 40°S below a depth of 3 km, which is calculated using an ideal age tracer, increases from 400 years in simulation 1 to 1700 years in simulation 2. A similar increase of deep Southern Ocean ventilation age has been observed between the present and LGM [*Skinner et al.*, 2010], and the simulated vertical gradient of ventilation age in the mid-depth Southern Ocean water column also fits glacial observation [*Burke and Robinson*, 2012]. The decline in atmospheric $\Delta^{14}C$ of 130 permil from simulation 2 to simulation 1 is also consistent with the rapid decline in atmospheric $\Delta^{14}C$ upon deglaciation [*Reimer et al.*, 2009], a portion of which has

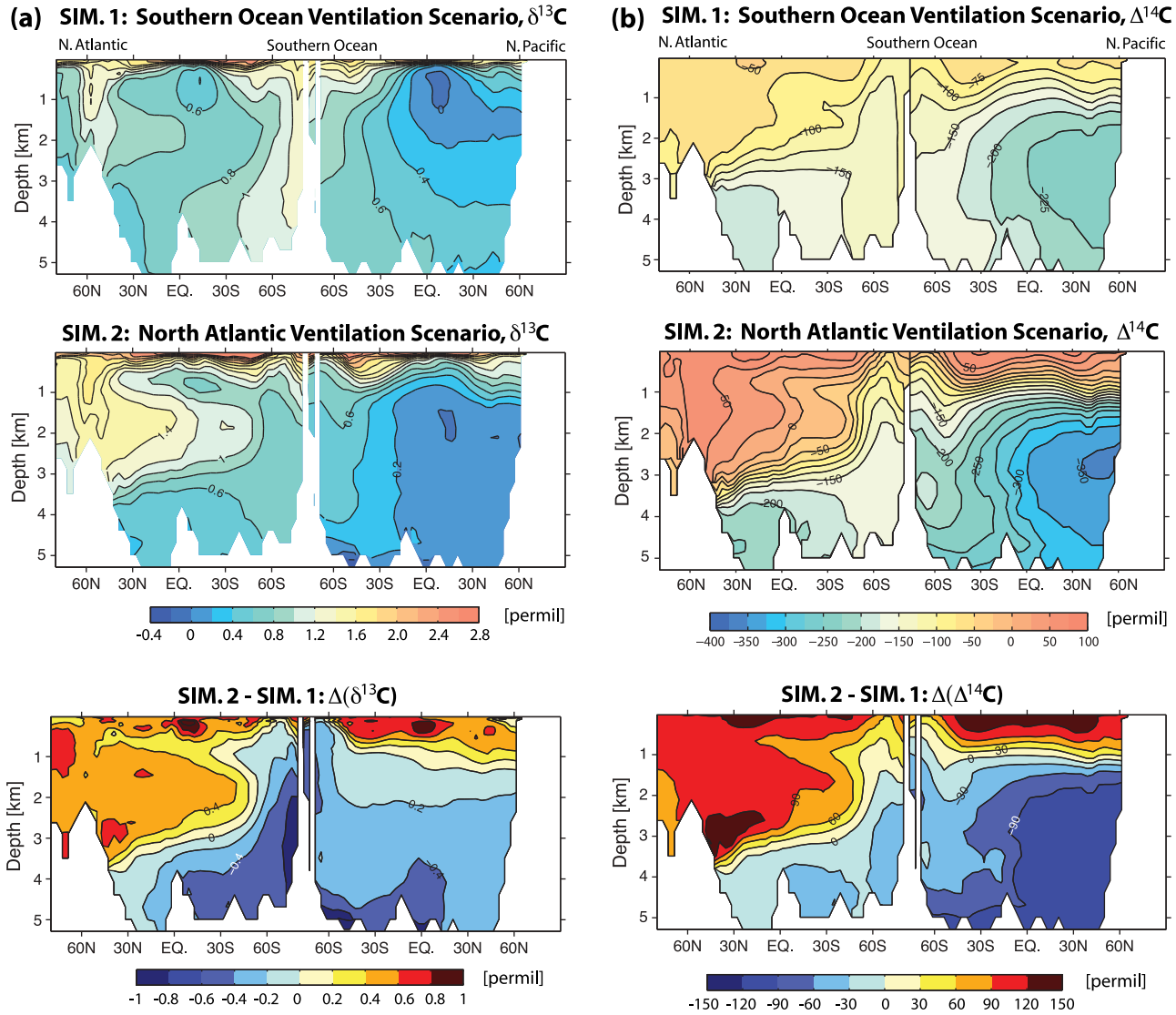

Figure 3. Carbon isotope distributions. (a) The distributions of $\delta^{13}C$ for simulation 1 (top panel) and simulation 2 (middle panel). The difference between simulation 2 and simulation 1 is presented in bottom panel. Atmospheric $\delta^{13}C$ is −6.48 permil in simulation 1 and −5.91 permil in simulation 2 when the total amounts of ^{13}C and ^{12}C are conserved in the ocean-atmosphere system. Zonally averaged fields are presented for the Atlantic and Pacific oceans. (b) Same as Figure 3a except that the distributions of $\Delta^{14}C$ are presented. Atmospheric $\Delta^{14}C$ is 0 permil in simulation 1 and 130 permil in simulation 2 when the atmospheric production rate is fixed.

been attributed to the deglacial acceleration in deep ocean ventilation rate [*Hughen et al.*, 1998, 2004; *Muscheler et al.*, 2004; *Skinner et al.*, 2010; *Marchitto et al.*, 2007; *Hain et al.*, 2011; *Burke and Robinson*, 2011].

[17] The sensitivity of atmospheric $\Delta^{14}C$ change with respect to changes in ocean ventilation rate depends also on the absolute size of the global ^{14}C inventory. If we adopt a 30% greater production rate (as suggested by *Köhler et al.* [2006] for the LGM) for both our simulations, the difference of atmospheric $\Delta^{14}C$ between simulation 1 and simulation 2 also rises by roughly 30%, from 130 permil to 177 permil. Thus, including the effect of a greater ^{14}C inventory suggests that a substantial part, if not all, of the ∼190 permil deglacial atmospheric $\Delta^{14}C$ decline [*Reimer et al.*, 2009; *Broecker and Barker*, 2007] may be explained by more rapid ocean ventilation during deglaciations [see also *Hughen et al.*, 2004].

[18] Finally, we note that the concentration of dissolved oxygen declines only moderately from simulation 1 to simulation 2 (Figure 5) despite the fact that the ventilation rate of the global deep ocean declines quite substantially. In that sense, simulation 2 agrees with reconstructions that indicate greater than modern deep ocean oxygen depletion during the LGM (greater authigenic uranium content of pelagic sediments) but the absence of bottom water anoxia (e.g., absence of molybdenum enrichment) [*Galbraith et al.*, 2007; *Jaccard et al.*, 2009; *Jaccard and Galbraith*, 2012]. The overall lower concentration of dissolved oxygen in simulation 2 is a direct consequence of the more efficient soft-tissue pump and the concomitant increase in the

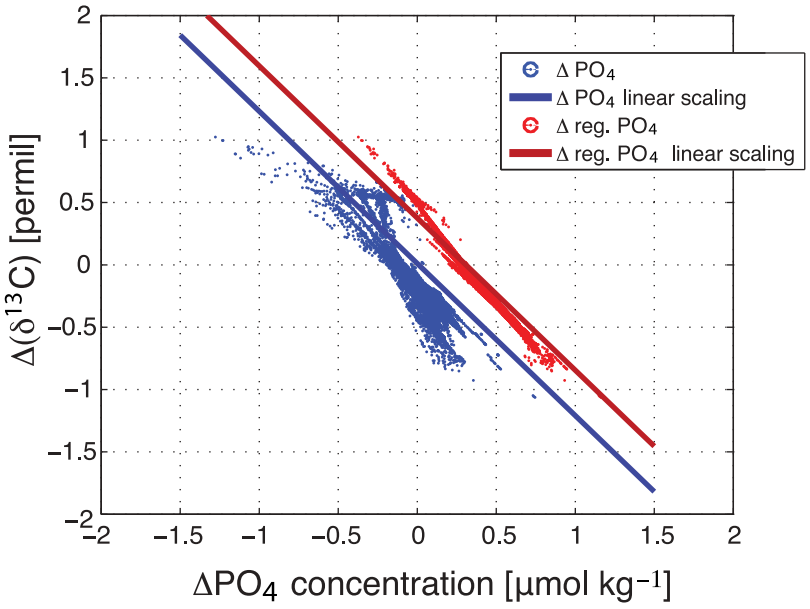

Figure 4. A scatterplot of PO_4 versus $\delta^{13}C$, taken from the model grids below 2000 m of the global ocean. Blue dots represent ΔPO_4 versus $\Delta\delta^{13}C$ where Δ denotes the difference between simulation 2 and simulation 1 (i.e., simulation 2 minus simulation 1). Blue line represents a linear scaling of $\Delta\delta^{13}C = -20 \cdot 137/2250(\Delta PO_4)$ where -20 is the fractionation factor of $\delta^{13}C$ during photosynthesis, 137 is the stoichiometric ratio of C:P in the model, and 2250 μmol kg^{-1} is the mean concentration of dissolved inorganic carbon in the model ocean. This linear scaling is adapted from *Broecker and Maier-Reimer* [1992]. Red dots represent $\Delta reg.\ PO_4$ versus $\Delta\delta^{13}C$ where *reg.* PO_4 is the regenerated PO_4. Red line represents a modified linear scaling of $\Delta\delta^{13}C = -20 \cdot 137/2250(\Delta reg.\ PO_4 - \Delta\langle reg.\ PO_4\rangle)$ where $\Delta\langle reg.\ PO_4\rangle = 0.31$ μmol kg^{-1} is a difference in the mean value of regenerated PO_4 between simulation 2 and simulation 1. The idea for the modified scaling is that we replace PO_4 and the mean $\langle PO_4\rangle$ in the original scaling of *Broecker and Maier-Reimer* [1992] with regenerated PO_4. The linear scaling represents the $\delta^{13}C$ change that would occur if there were no air-sea gas exchange effect on $\delta^{13}C$.

concentration of respired carbon: changing from simulation 1 to simulation 2, ~0.3 μmol kg^{-1} of preformed phosphate become regenerated, thereby raising the globally averaged concentration of sequestered carbon by 43 μmol kg^{-1} and depleting dissolved oxygen by 57 μmol kg^{-1} (the globally averaged concentration of dissolved oxygen declines from 207 μmol kg^{-1} in simulation 1 to 150 μmol kg^{-1} in simulation 2). The majority of this change to more efficient biological carbon sequestration can be attributed to the volumetric expansion of water last ventilated in the North Atlantic (see the Appendix section).

[19] The principle reason that oxygen declines less than one might have predicted for the substantial aging of the deep ocean is the decline in ocean productivity: lower productivity, especially in the Antarctic, acts to reduce the bulk deep ocean rate of oxygen consumption caused by the respiration of organic matter. Thus, while the reduction of southern-sourced overturning slows the supply of oxygen to the abyss, the simulated decline of Antarctic productivity (which is consistent with observations [*François et al.*, 1997; *Frank et al.*, 2000; *Kumar et al.*, 1993; *Mortlock et al.*, 1991; *Kohfeld et al.*, 2005]) reduces the deep ocean oxygen demand. To further illustrate this point, we calculate the ratio of apparent oxygen utilization (AOU) and the ideal ventilation age for water below 2 km depth. This metric of bulk deep ocean oxygen utilization rate declines from 0.15 μmol kg^{-1} yr^{-1} (120 μmol kg^{-1} of AOU divided by an ideal ventilation age of 800 years) in simulation 1 to 0.09 μmol kg^{-1} yr^{-1} (200 μmol kg^{-1} divided by an age of 2200 years) in simulation 2. Indeed, there is supporting observational evidence for a reduced glacial respiration rate [*Bryan et al.*, 2011; S. P. Bryan et al., Constraints on deep ocean organic carbon remineralization rates during the Last Glacial Maximum, manuscript in preparation, 2012]. Nonetheless, despite the reduced rate of oxygen consumption in simulation 2, we find small patches of hypoxic (≤60 μmol kg^{-1} O_2) bottom water (Figure 5) with an ideal ventilation age of 2400 years and an apparent ^{14}C ventilation age of 3100 years (i.e., a 31% depletion of $^{14}C/^{12}C$ relative to the $^{14}C/C$ of the concurrent atmosphere). This relationship between oxygen utilization, ventilation age and $^{14}C/C$ depletion is similar to that obtained in the box model simulations of *Hain et al.* [2011] where, in the context of a less productive glacial ocean, the onset of bottom water anoxia occurred at an ideal ventilation age of little more than 3000 years.

[20] Our analysis of the simulated oxygen distribution has two conceptually important implications. First, the coupling between regenerated nutrients, deep ocean sequestration of respired carbon and deep ocean oxygen depletion poses an upper limit on the contribution of the soft-tissue pump to glacial CO_2 drawdown: for the deep ocean to remain fairly

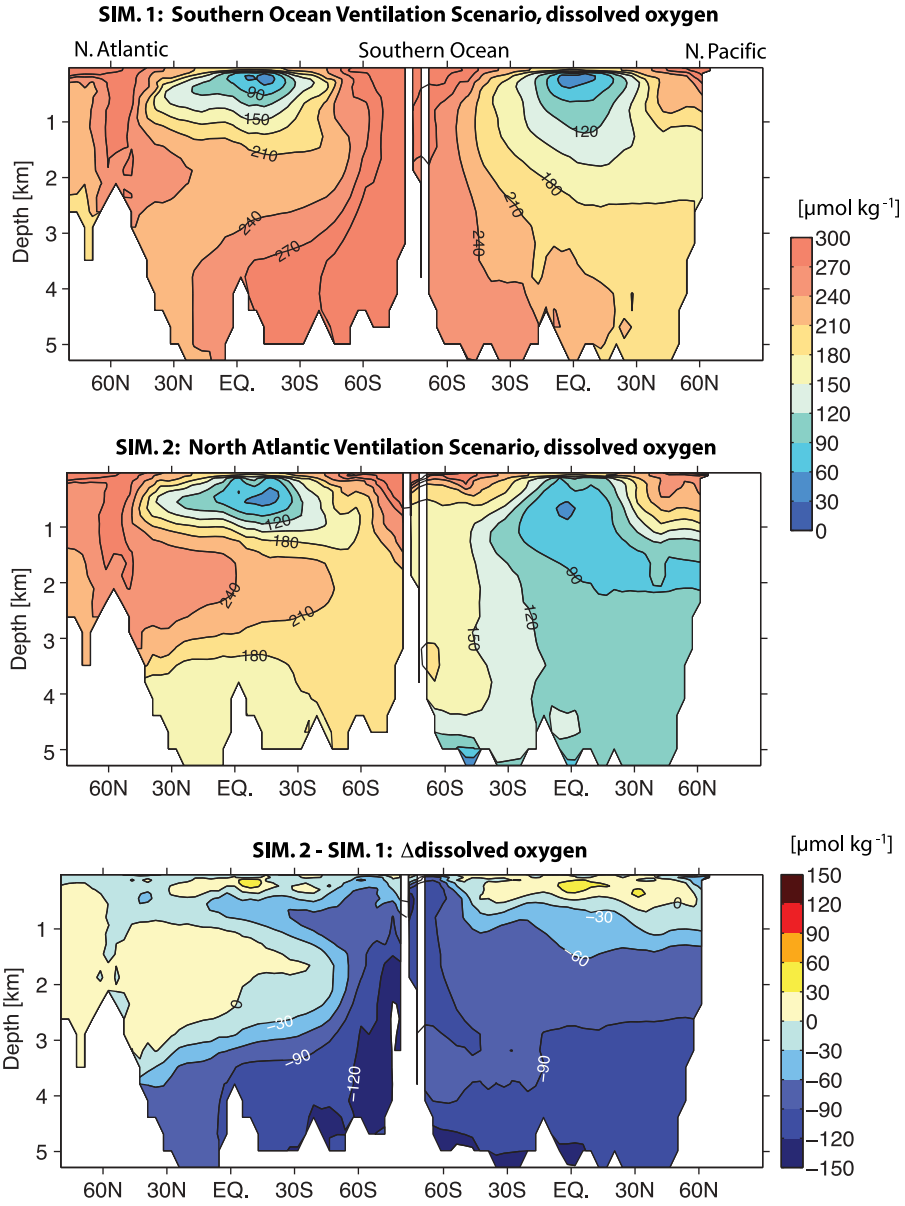

Figure 5. Dissolved oxygen distributions. The distributions of dissolved oxygen for (top) simulation 1 and (middle) simulation 2. (bottom) The difference between simulation 2 and simulation 1 is shown. Zonally averaged fields are presented for the Atlantic and Pacific oceans. Units are μmol kg^{-1}.

well oxygenated in any given glacial model scenario (e.g., *Toggweiler* [1999], *Hain et al.* [2010], and this study's simulation 2), only roughly half of the glacial CO_2 drawdown may be achieved by increased efficiency in the soft-tissue pump. Therefore, the remainder of CO_2 drawdown must be attributed to other processes, with an increase of ocean alkalinity arguably being the most important [e.g., *Sigman et al.*, 2010]. Second, of the two scenarios described by *Broecker and Clark* [2010], simulation 2 agrees better with their "Slow Ventilation Scenario" than with their "Isolated Abyssal Reservoir Scenario". Instead of highly localized biological carbon sequestration into a stagnant, uniquely ^{14}C-deplete abyssal bottom layer, the glacial scenario presented here suggests that the entrainment of North Atlantic-ventilated water into the deep glacial ocean allowed carbon sequestration to be broadly distributed across the entire deep ocean, thereby reducing atmospheric CO_2 while retaining well oxygenated bottom waters.

4. Discussion and Conclusions

[21] Reduced escape of carbon dioxide, through a reduction in the deep ocean ventilation from the Southern Ocean, is arguably the most popular hypothesis for lowering atmospheric CO_2 to glacial levels, with support from both observations and models. However, implicit in this hypothesis is the need for the glacial North Atlantic to have taken over the ventilation of a great fraction of the ocean interior,

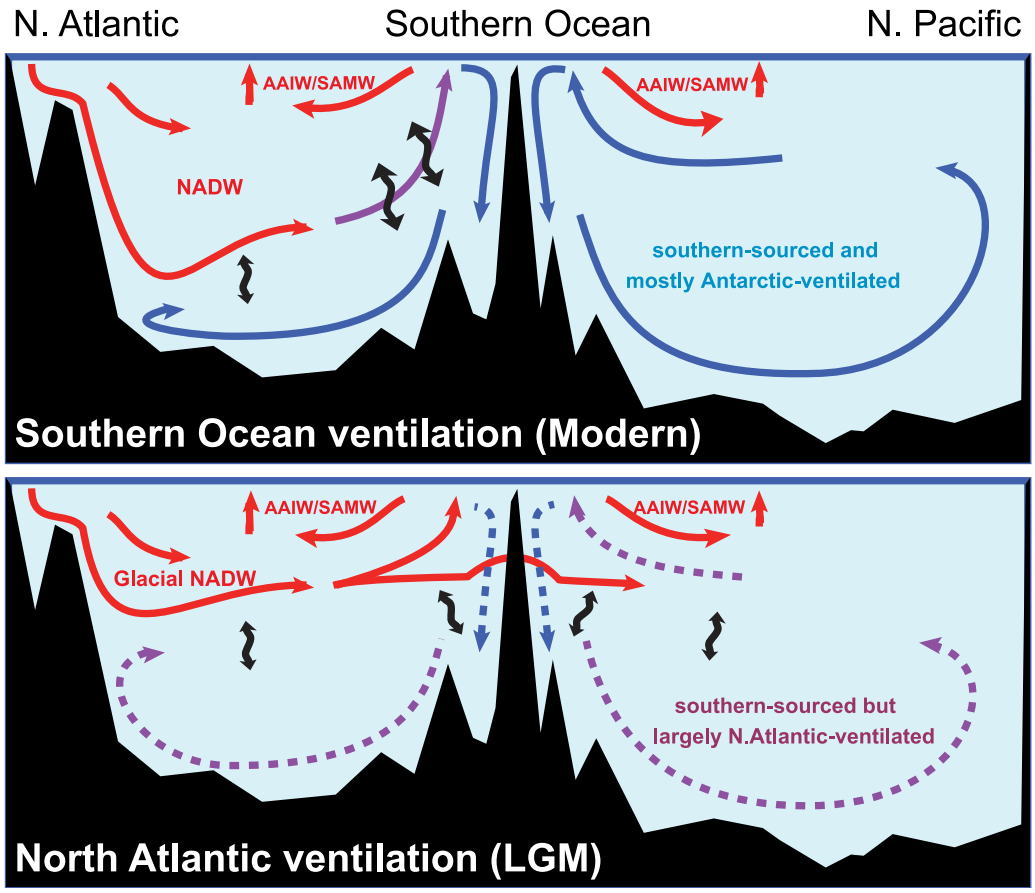

Figure 6. Schematics of ocean circulation for (top) the interglacial time and (bottom) the last glacial maximum, as inferred from our simulations. Red and blue solid lines represent flow of water with low and high concentrations of preformed nutrients, respectively. Purple solid line represents a mixture of water masses with high and low preformed nutrients. Blue and purple dotted lines represent flows with their intensities weakened relative to the corresponding solid lines. Wavy black double-headed arrows represent mixing and entrainment. This cartoon shows that the North Atlantic-ventilated water increasingly dominates the global abyss as the overturning circulation of the Southern Ocean weakens.

and this requirement has been seen as in direct conflict with a large body of paleoceanographic data showing the glacial expansion of southern-sourced water in the deep Atlantic. This study proposes a way out of this puzzle, showing the plausibility of a circulation pattern in which the poorly ventilated glacial deep ocean is filled with dense water that is southern-sourced but nevertheless contains an increased fraction of the North Atlantic-ventilated water. A comparison between the idealized model experiments reveals that the entrainment of NADW into the abyss associated with the reduced overturning circulation of the Southern Ocean can simultaneously produce low levels of atmospheric CO_2, low $^{13}C/^{12}C$ and $^{14}C/C$ in bottom waters, and elevated atmospheric $\Delta^{14}C$. In this regard, our hypothesized glacial ocean circulation pattern, which is schematized in Figure 6, reconciles the drawdown of atmospheric pCO_2 with the reconstructed volumetric expansion of the southern-sourced deep water during glacial times.

[22] According to our glacial-like simulation (simulation 2), the low $^{13}C/^{12}C$ of southern-sourced deep water stems not from the expansion of water last ventilated in the polar Antarctic surface [*Skinner*, 2009] but rather from the reduced rate at which respired carbon is brought up to the surface to be vented to the atmosphere. An equivalent explanation for the $\delta^{13}C$ drop is that it reflects greater deep ocean storage of respired carbon associated with a shift of deeply held nutrients from being preformed to regenerated, a consequence of an increase in the importance of the North Atlantic in abyssal water ventilation [*Toggweiler et al.*, 2003; *Marinov et al.*, 2008a].

[23] While the difference in vertical diffusivity that gives rise to the changes in our two simulations was not motivated by observations or theoretical arguments for a physical mechanism that might drive such a change in the diffusivity, the remarkable agreement between our contrasting model simulations and the corresponding glacial and interglacial carbon isotopes and air-sea CO_2 observations suggests that our simulations may have captured essential components of how the ocean actually did change even if the specific mechanism we used to drive those changes may not be

realistic. We note that candidate mechanisms have been described in the literature, including an equatorward shift in the Southern Hemisphere westerlies [*Toggweiler et al.*, 2006], increased Southern Ocean stratification due to cooling of NADW [*Gildor and Tziperman*, 2001] and the global ocean [*De Boer et al.*, 2007] and changing impacts of brine rejection associated with changes in sea ice production and/or ice shelf extent [*Adkins et al.*, 2002; *Bouttes et al.*, 2010]. Further investigation of this issue is required.

[24] The mechanisms and pathways through which the entrainment of NADW into the global abyss occurs remain an area of active research. Future work should explore the ventilation volume hypothesis in a more realistic model framework that accounts for the interactions among the ocean, atmosphere, seafloor and sea ice, and paleoceanographic reconstructions that speak to the physical state of the ocean (i.e., foraminiferal $\delta^{18}O$) will offer crucial constraints to distinguish between physical mechanisms. However, beyond the shortcomings of our simulations, we note that there are two distinct ways that glacial North Atlantic-ventilated water could have found its way into the deep ocean (Figure 6): (1) NADW is entrained around Antarctica into descending, newly formed glacial AABW, and (2) despite low vertical diffusivity, NADW mixes downward from mid-depth into the slowly circulating deep ocean. With regard to the latter, downward mixing of NADW would have been encouraged because the areal extent of the interface between glacial NADW and glacial AABW was much greater than the modern areal extent between NADW and AABW in the Atlantic [*Lund et al.*, 2011] and likely extended through much of the Indo-Pacific basin [*Lynch-Stieglitz et al.*, 1996]. With the slower replacement rate of abyssal water from the Southern Ocean surface, any processes that led to entrainment of NADW may have become proportionally more important in forming the southern-sourced deep water. In any case, this study suggests that substantial ventilation of the deep glacial ocean from the North Atlantic surface is a plausible circulation scenario in the context of observed carbon isotope distributions for glacial times.

Appendix A: The Ventilation Volume Effect of Atmospheric pCO_2 Change

[25] We estimate atmospheric pCO_2 change driven by the change in the volume fractions of the global ocean ventilated from the North Atlantic and the Southern Ocean, under the assumption that surface nutrient distribution remains unchanged. Using a Green's function approach, we obtain the globally averaged concentration of preformed PO_4 for simulation 1 (SIM1) as

$$\overline{[PO_4]_{pref}^{SIM1}} = \frac{1}{M_o}\int_{\Omega} PO_4\,(r_s)^{SIM1}\cdot G(r_s)^{SIM1} d^2 r_s, \qquad \text{(A1)}$$

where M_o denotes the total mass of the global ocean and where the global inventory of preformed PO_4 is obtained by integrating the convolution of surface PO_4 ($PO_4(r_s)$) and the volume integrated Green's function ($G(r_s)$) over the entire surface ocean (Ω) [*Kwon et al.*, 2011; *Primeau*, 2005]. The globally averaged concentration of preformed PO_4 for simulation 1 is estimated to be 1.50 μmol kg^{-1}. Now, we assume that surface PO_4 distribution remains fixed at the value obtained from simulation 1 while the ocean circulation pattern changes from simulation 1 to simulation 2. The globally averaged concentration of preformed PO_4 in this case becomes 1.28 μmol kg^{-1}, which is obtained from

$$\overline{[PO_4]_{pref}^{SIM2}} = \frac{1}{M_o}\int_{\Omega} PO_4\,(r_s)^{SIM1}\cdot G(r_s)^{SIM2} d^2 r_s, \qquad \text{(A2)}$$

where the Green's function of simulation 2 is convolved with the nutrient distribution of simulation 1. The reduction in preformed PO_4 of 0.22 μmol kg^{-1} is attributed to the increased volume fraction of the global ocean ventilated from the North Atlantic (i.e., decreased volume fraction of the global ocean ventilated from the Southern Ocean) in simulation 2.

[26] *Kwon et al.* [2011] derived an analytical relationship between preformed nutrient reservoir and atmospheric pCO_2 change, which is

$$\frac{\Delta pCO_2}{pCO_2} = 0.0053\cdot r_{C:P}\cdot \Delta\overline{[PO_4]_{pref}}, \qquad \text{(A3)}$$

where $r_{C:P}$ denotes the stoichiometric ratio of C:P. Applying $r_{C:P}$ = 137 [*Kwon and Primeau*, 2008], the reference value for pCO_2 of 280 ppm and $\Delta\overline{[PO_4]_{pref}} = -0.22$ μmol kg^{-1}, the ventilation volume effect, ΔpCO_2, is -45 ppm.

[27] **Acknowledgments.** We thank Jess Adkins for the invaluable and constructive discussions while preparing this manuscript. We also thank Joellen Russell and Anand Gnanadesikan for useful comments. Comments from anonymous reviewers and the editor, Christopher Charles, also helped improve this manuscript. M.P.H and D.M.S. acknowledge support by the U.S. NSF, the German DFG, the Humboldt and MacArthur Foundations, and the Siebel Energy Grand Challenge and Walbridge Fund Award at Princeton E.Y.K. and J.L.S. acknowledge award ANT-1040957 from NSF and award NA07OAR4310096 from NOAA. The statements, findings, conclusions, and recommendations are those of the authors and do not necessarily reflect the views of the National Oceanic and Atmospheric Administration or the U.S. Department of Commerce.

References

Adkins, J. F., K. McIntyre, and D. P. Schrag (2002), The salinity, temperature, and $\delta^{18}O$ of the glacial deep ocean, *Science*, *298*, 1769–1773.

Anderson, L. A., and J. L. Sarmiento (1994), Redfield ratios of remineralization determined by nutrient data analysis, *Global Biogeochem. Cycles*, *8*(1), 65–80.

Archer, D. E., P. A. Martin, J. Milovich, V. Brovkin, G.-K. Plattner, and C. Ashendel (2003), Model sensitivity in the effect of Antarctic sea ice and stratification on atmospheric pCO_2, *Paleoceanography*, *18*(1), 1012, doi:10.1029/2002PA000760.

Bouttes, N., D. Paillard, and D. M. Roche (2010), Impact of brine-indueced stratification on the glacial carbon cycle, *Clim. Past*, *6*, 575–589, doi:10.5194/cp-6-575-2010.

Boyle, E. A., and L. Keigwin (1987), North Atlantic thermohaline circulation during the past 20,000 years linked to high-latitude surface temperature, *Nature*, *330*, 35–40.

Bradtmiller, L. I., R. F. Anderson, J. P. Sachs, and M. Q. Fleisher (2010), A deeper respired carbon pool in the glacial equatorial Pacific Ocean, *Earth Planet. Sci. Lett.*, *299*, 417–425, doi:10.1016/j.epsl.2010.09.022.

Broecker, W., and S. Barker (2007), A 190‰ drop in atmosphere's $\Delta^{14}C$ during the "Mystery Interval" (17.5 to 14.5 kyr), *Earth Planet. Sci. Lett.*, *256*, 90–99, doi:10.1016/j.epsl.2007.01.015.

Broecker, W., and E. Clark (2010), Search for a glacial-age ^{14}C-depleted ocean reservoir, *Geophys. Res. Lett.*, *37*, L13606, doi:10.1029/2010GL043969.

Broecker, W. S., and E. Maier-Reimer (1992), The influence of air and sea exchange on the carbon isotope distribution in the sea, *Global Biogeochem. Cycles*, *6*(3), 315–320, doi:10.1029/92GB01672.

Broecker, W. S., and T.-H. Peng (1987), The role of $CaCO_3$ compensation in the glacial to interglacial atmospheric CO_2 change, *Global Biogeochem. Cycles*, *1*(1), 15–29.

Broecker, W. S., T. Takahashi, and T. Takahashi (1985), Sources and flow patterns of deep-ocean waters as deduced from potential temperature, salinity, and initial phosphate concentration, *J. Geophys. Res.*, *90*(C4), 6925–6939.

Broecker, W. S., et al. (1998), How much deep water is formed in the Southern Ocean?, *J. Geophys. Res.*, *103*(C8), 15,833–15,843.

Bryan, S. P., S. J. Lehman, and T. M. Marchitto (2011), The relationship between $\Delta^{14}C$ and $\delta^{13}C$ of DIC in the LGM Ocean, *Mineral. Mag.*, *75*(3), 590.

Burke, A., and L. F. Robinson (2012), The Southern Ocean's role in carbon exchange during the last deglaciation, *Science*, *335*, 557–561, doi:10.1126/science.1208163.

Curry, W. B., and D. W. Oppo (2005), Glacial water mass geometry and the distribution of $\delta^{13}C$ of ΣCO_2 in the western Atlantic Ocean, *Paleoceanography*, *20*, PA1017, doi:10.1029/2004PA001021.

De Boer, A. M., D. M. Sigman, J. R. Toggweiler, and J. L. Russell (2007), Effect of global ocean temperature change on deep ocean ventilation, *Paleoceanography*, *22*, PA2210, doi:10.1029/2005PA001242.

DeVries, T., and F. Primeau (2009), Atmospheric pCO_2 sensitivity to the solubility pump: Role of the low-latitude ocean, *Global Biogeochem. Cycles*, *23*, GB4020, doi:10.1029/2009GB003537.

DeVries, T., and F. Primeau (2011), Dynamically and observationally constrained estimates of water-mass distributions and ages in the Global Ocean, *J. Phys. Oceanogr.*, *41*, 2381–2401.

Downes, S. M., A. Gnanadesikan, S. M. Griffies, and J. L. Sarmiento (2011), Water mass exchange in the Southern Ocean in coupled climate models, *J. Phys. Oceanogr.*, *41*, 1756–1771.

Duplessy, J. C., N. J. Shackleton, R. G. Fairbanks, L. Labeyrie, D. Oppo, and N. Kallel (1988), Deepwater source variations during the last climatic cycle and their impact on the global deepwater circulation, *Paleoceanography*, *3*(3), 343–360, doi:10.1029/PA003i003p00343.

Elderfield, H., and R. E. M. Rickaby (2000), Oceanic Cd/P ratio and nutrient utilization in the glacial Southern Ocean, *Nature*, *405*, 305–310.

François, R., et al. (1997), Contribution of Southern Ocean surface-water stratification to low atmospheric CO_2 concentrations during the last glacial period, *Nature*, *389*, 929–935.

Frank, M., et al. (2000), Similar glacial and interglacial export bioproductivity in the Atlantic Sector of the Southern Ocean: Multiproxy evidence and implications for glacial atmospheric CO_2, *Paleoceanography*, *15*(6), 642–658, doi:10.1029/2000PA000497.

Galbraith, E. D., et al. (2007), Carbon dioxide release from the North Pacific abyss during the last deglaciation, *Nature*, *449*, 890–893.

Gebbie, G., and P. Huybers (2010), Total matrix intercompasiron: A method for determining the geometry of water-mass pathways, *J. Phys. Oceanogr.*, *40*, 1710–1728.

Gebbie, G., and P. Huybers (2011), How is the ocean filled?, *Geophys. Res. Lett.*, *38*, L06604, doi:10.1029/2011GL046769.

Gent, P. R., and J. C. McWilliams (1990), Isopycnal mixing in ocean circulation models, *J. Phys. Oceanogr.*, *20*, 150–155.

Gildor, H., and E. Tziperman (2001), Physical mechanisms behind biogeochemical glacial-interglacial CO_2 variations, *Geophys. Res. Lett.*, *28*, 2421–2424.

Hain, M. P., D. M. Sigman, and G. H. Haug (2010), Carbon dioxide effects of Antarctic stratification, North Atlantic Intermediate Water formation, and subantarctic nutrient drawdown during the last ice age: Diagnosis and synthesis in a geochemical box model, *Global Biogeochem. Cycles*, *24*, GB4023, doi:10.1029/2010GB003790.

Hain, M. P., D. M. Sigman, and G. H. Haug (2011), Shortcomings of the isolated abyssal reservoir model for deglacial radiocarbon changes in the mid-depth Indo-Pacific Ocean, *Geophys. Res. Lett.*, *38*, L04604, doi:10.1029/2010GL046158.

Hughen, K. A., et al. (1998), Deglacial changes in ocean circulation from an extended radiocarbon calibration, *Nature*, *391*, 65–68.

Hughen, K. A., et al. (2004), ^{14}C activity and global carbon cycle changes over the past 50,000 years, *Science*, *303*, 202–207.

International Union of Pure and Applied Chemistry (1999), Isotopic compositions of the elements 1997, *Pure Appl. Chem.*, *71*, 1593–1607.

Ito, T., and M. J. Follows (2005), Preformed phosphate, soft tissue pump and atmospheric CO_2, *J. Marine Res.*, *63*, 813–839.

Iudicone, D., S. Speich, G. Madec, and B. Blanke (2008), The Global Conveyor Belt from a Southern Ocean perspective, *J. Phys. Oceanogr.*, *38*, 1401–1425.

Jaccard, S. L., and E. D. Galbraith (2012), Large climate-driven changes of oceanic oxygen concentrations during the last deglaciation, *Nat. Geosci.*, *5*, 151–156, doi:10.1038/ngeo1352.

Jaccard, S. L., et al. (2009), Subarctic Pacific evidence for a glacial deepening of the oceanic respired carbon pool, *Earth Planet. Sci. Lett.*, *277*, 156–165.

Johnson, G. C. (2008), Quantifying Antarctic Bottom water and North Atlantic Deep Water volumes, *J. Geophys. Res.*, *113*, C05027, doi:10.1029/2007JC004477.

Knox, F., and M. B. McElroy (1984), Changes in atmospheric CO_2: Influence of the marine biota at high latitude, *J. Geophys. Res.*, *89*, 4629–4637.

Kohfeld, K. E., C. L. Quéré, S. P. Harrison, and R. F. Anderson (2005), Role of marine biology in glacial-interglacial CO_2 cycles, *Science*, *308*, 74–78, doi:10.1126/science.1105375.

Köhler, P., and H. Fischer (2006), Simulating low frequency changes in atmospheric CO_2 during the last 740,000 years, *Clim. Past*, *2*, 57–78.

Köhler, P., R. Muscheler, and H. Fischer (2006), A model-based interpretation of low frequency changes in the carbon cycle during the last 120,000 years and its implications for the reconstruction of atmospheric $\Delta^{14}C$, *Geochem. Geophys. Geosyst.*, *7*, Q11N06, doi:10.1029/2005GC001228.

Kumar, N., R. Gwiazda, R. F. Anderson, and P. N. Froelich (1993), $^{231}Pa/^{230}Th$ ratios in sediments as a proxy for past changes in Southern Ocean productivity, *Nature*, *362*, 45–48, doi:10.1038/362045a0.

Kwon, E. Y., and F. Primeau (2008), Optimization and sensitivity of a global biogeochemistry ocean model using combined in situ DIC, alkalinity, and phosphate data, *J. Geophys. Res.*, *113*, C08011, doi:10.1029/2007JC004520.

Kwon, E. Y., J. L. Sarmiento, J. R. Toggweiler, and T. DeVries (2011), The control of atmospheric pCO_2 by ocean ventilation change: The effect of the oceanic storage of biogenic carbon, *Global Biogeochem. Cycles*, *25*, GB3026, doi:10.1029/2011GB004059.

Large, W. C., J. C. McWilliams, and S. C. Doney (1994), Oceanic vertical mixing: A review and a model with a nonlocal boundary layer parameterization, *Rev. Geophys.*, *32*, 363–403.

Lisiecki, L. E. (2010), A simple mixing explanation for late Pleistocene changes in the Pacific-South Atlantic benthic $\delta^{13}C$ gradient, *Clim. Past*, *6*, 305–314.

Lund, D. C., J. F. Adkins, and R. Ferrari (2011), Abyssal Atlantic circulation during the Last Glacial Maximum: Constraining the ratio between transport and vertical mixing, *Paleoceanography*, *26*, PA1213, doi:10.1029/2010PA001938.

Lynch-Stieglitz, J., T. F. Stocker, W. S. Brocker, and R. G. Fairbanks (1995), The influence of air-sea exchange on the isotopic composition of oceanic carbon: Observations and modelling, *Global Bigeochem. Cycles*, *9*, 653–665.

Lynch-Stieglitz, J., A. van Geen, and R. G. Fairbanks (1996), Interocean exchange of glacial North Atlantic Intermediate Water: Evidence from subantarctic Cd/Ca and carbon isotope measurements, *Paleoceanography*, *11*(2), 191–201.

Lynch-Stieglitz, J., et al. (2007), Atlantic meridional overturning circulation during the Last Glacial Maximum, *Science*, *316*, 66–69.

Marchitto, T. M., and W. S. Broecker (2006), Deep water mass geometry in the glacial Atlantic Ocean: A review of constraints from the paleonutrient proxy Cd/Ca, *Geochem. Geophys. Geosyst.*, *7*, Q12003, doi:10.1029/2006GC001323.

Marchitto, T. M., S. J. Lehman, J. D. Ortiz, J. Flückiger, and A. van Geen (2007), Marine radiocarbon evidence for the mechanism of deglacial atmospheric CO_2 rise, *Science*, *316*, 1456–1459.

Marinov, I., M. J. Follows, A. Gnandesikan, J. L. Sarmiento, and R. D. Slater (2008a), How does ocean biology affect atmospheric pCO_2? Theory and models, *J. Geophys. Res.*, *113*, C07032, doi:10.1029/2007JC004598.

Marinov, I., A. Gnanadesikan, J. L. Sarmiento, J. R. Toggweiler, and B. Mignone (2008b), Impact of oceanic circulation on the ocean biological carbon storage and atmospheric pCO_2, *Global Biogeochem. Cycles*, *22*, GB3007,doi:10.1029/2007GB002958.

Mortlock, R. A., et al. (1991), Evidence for lower productivity in the Antarctic Ocean during the last glaciation, *Nature*, *351*, 220–223, doi:10.1038/351220a0.

Muscheler, R., et al. (2004), Changes in the carbon cycle during the last deglaciation as indicated by the comparison of ^{10}Be and ^{14}C records, *Earth Planet. Sci. Lett.*, *219*, 325–340.

Najjar, R. G., et al. (2007), Impact of circulation on export production, dissolved organic matter, and dissolved oxygen in the ocean: Results from Phase II of the Ocean Carbon-cycle Model Intercomparison Project (OCMIP-2), *Global Biogeochem. Cycles*, *21*, GB3007, doi:10.1029/2006GB002857.

Ninnemann, U. S., and C. D. Charles (2002), Changes in the mode of Southern Ocean circulation over the last glacial cycle revealed by foraminiferal stable isotopic variability, *Earth Planet. Sci. Lett.*, *201*, 383–396.

Olsson, I. U. (1970), The use of oxalic acid as a standard, in *Radiocarbon Variations and Absolute Chronology*, edited by I. U. Olsson, p. 17, Wiley Intersci., New York.

Orsi, A. H., G. C. Johnson, and J. L. Bullister (1999), Circulation, mixing, and production of Antarctic Bottom Water, *Prog. Oceanogr.*, *43*, 55–109.

Petit, J. R., et al. (1999), Climate and atmospheric history of the past 420,000 years from the Vostok ice core, Antarctica, *Nature*, *399*, 429–436.

Piotrowski, A. M., S. L. Goldstein, S. R. Hemming, and R. G. Fairbanks (2005), Temporal relationships of carbon cycling and ocean circulation at glacial bondaries, *Science*, *307*, 1933–1938.

Price, J. F., and M. O. Baringer (1994), Outflows and deep water production by marginal seas, *Prog. Oceanog.*, *33*, 161–200.

Primeau, F. (2005), Characterizing transport between the surface mixed layer and the ocean interior with a forward and adjoint global ocean transport model, *J. Phys. Oceanogr.*, *35*, 545–564.

Redfield, A. C. (1942), The processes determining the concentration of oxygen, phosphate, and other organic derivatives within the depths of the Atlantic Ocean, *Pap. Phys. Oceanogr. Meteorol.*, *9*(2), 22 pp.

Reimer, P. J., et al. (2009), IntCal09 and Marine09 radiocarbon age calibration curves, 0–50,000 years cal BP, *Radiocarbon*, *51*(4), 1111–1150.

Robinson, L. F., et al. (2005), Radiocarbon variability in the western north Atlantic during the last deglaciation, *Science*, *310*, 1469–1473.

Robinson, R. S., and D. M. Sigman (2008), Nitrogen isotopic evidence for a poleward decrease in surface nitrate within the ice age Antarctic, *Quat. Sci. Rev.*, *27*(9–10), 1076–1090.

Rutberg, R. L., S. R. Hemming, and S. L. Goldstein (2000), Reduced North Atlantic Deep Water to the glacial Southern Ocean inferred from neodymium isotope ratios, *Nature*, *405*, 935–938.

Sarmiento, J. L., and J. R. Toggweiler (1984), A new model for the role of the oceans in determining atmospheric pCO_2, *Nature*, *308*, 621–624.

Schmittner, A., and E. D. Galbraith (2008), Glacial greenhouse-gas fluctuations controlled by ocean circulation changes, *Nature*, *456*, 373–376, doi:10.1038/nature07531.

Siegenthaler, U., and T. Wenk (1984), Rapid atmospheric CO_2 variations and ocean circulation, *Nature*, *308*, 624–626.

Sigman, D. M., and E. A. Boyle (2000), Gacial/interglacial variations in atmospheric carbon dioxide, *Nature*, *407*, 859–869.

Sigman, D. M., and G. H. Haug (2003), Biological pump in the past, in *Treatise On Geochemistry*, edited by H. D. Holland and K. K. Turekian, pp. 491–528, Elsevier Sci., Oxford, U. K.

Sigman, D. M., M. P. Hain, and G. H. Haug (2010), The polar ocean and glacial cycles in atmospheric CO_2 concentration, *Nature*, *466*, 47–55.

Skinner, L. C. (2009), Glacial-interglacial atmospheric CO_2 change: A possible "standing volume" effect on deep-ocean carbon sequestration, *Clim. Past*, *5*, 537–550.

Skinner, L. C., S. Fallon, C. Waelbroeck, E. Michel, and S. Barker (2010), Ventilation of the deep Southern Ocean and deglacial CO_2 rise, *Science*, *328*(5982), 1147–1151.

Speer, K., S. R. Rintoul, and B. Sloyan (2000), The diabatic Deacon cell, *J. Phys. Oceanogr.*, *30*, 3212–3222.

Stephens, B. B., and R. F. Keeling (2000), The influence of Antarctic sea ice on glacial-interglacial CO_2 variations, *Nature*, *404*, 171–174.

Stuiver, M., and H. A. Polach (1977), Discussion reporting of ^{14}C data, *Radiocarbon*, *19*(3), 355–363.

Takahashi, T., W. S. Broecker, and S. Langer (1985), Redfield ratio based on chemical data from isopycnal surfaces, *J. Geophys. Res.*, *90*, 6907–6924, doi:10.1029/JC090iC04p06907.

Thornalley, D. J. R., S. Barker, W. S. Broecker, H. Elderfield, and I. N. McCave (2011), The deglacial evolution of North Atlantic deep convection, *Science*, *331*, 202–205.

Toggweiler, J. R. (1999), Variation of atmospheric CO_2 by ventilation of the ocean's deepest water, *Paleoceanography*, *14*(5), 571–588.

Toggweiler, J. R., R. Murnane, S. Carson, A. Gnanadesikan, and J. L. Sarmiento (2003), Representation of the carbon cycle in box models and GCMs, 2, Organic pump, *Global Biogeochem. Cycles*, *17*(1), 1027, doi:10.1029/2001GB001841.

Toggweiler, J. R., J. L. Russell, and S. Carson (2006), Midlatitude westerlies, atmospheric CO_2, and climate change during the ice ages, *Paleoceanography*, *21*, PA2005, doi:10.1029/2005PA001154.

Tziperman, E. (1986), On the role of interior mixing and air-sea fluxes in determining the stratification and circulation of the oceans, *J. Phys. Oceanogr.*, *16*, 680–693.

Walin, G. (1982), On the relation between sea-surface heat flow and thermal circulation in the ocean, *Tellus*, *34*, 187–195.